OPEN ACCESS

KING'S College LONDON

King's Research Portal

DOI:
10.1016/j.colsurfa.2019.05.056

Document Version
Peer reviewed version

Link to publication record in King's Research Portal

Citation for published version (APA):
Nascimento, J. U., Zambuzi, G. C., Ferreira, J. O. F., Paula, J. H., Ribeiro, T. S., Souza, A. L., Dreiss, C., Silva, L. L., & Francisco, K. R. (2019). A simple process to tune wettability of pectin-modified silanized glass. *COLLOIDS AND SURFACES A PHYSICOCHEMICAL AND ENGINEERING ASPECTS*, *577*, 67-74. https://doi.org/10.1016/j.colsurfa.2019.05.056

Citing this paper
Please note that where the full-text provided on King's Research Portal is the Author Accepted Manuscript or Post-Print version this may differ from the final Published version. If citing, it is advised that you check and use the publisher's definitive version for pagination, volume/issue, and date of publication details. And where the final published version is provided on the Research Portal, if citing you are again advised to check the publisher's website for any subsequent corrections.

General rights
Copyright and moral rights for the publications made accessible in the Research Portal are retained by the authors and/or other copyright owners and it is a condition of accessing publications that users recognize and abide by the legal requirements associated with these rights.

•Users may download and print one copy of any publication from the Research Portal for the purpose of private study or research.
•You may not further distribute the material or use it for any profit-making activity or commercial gain
•You may freely distribute the URL identifying the publication in the Research Portal

Take down policy
If you believe that this document breaches copyright please contact librarypure@kcl.ac.uk providing details, and we will remove access to the work immediately and investigate your claim.

Download date: 04. May. 2023

A SIMPLE PROCESS TO TUNE WETTABILITY OF PECTIN-MODIFIED SILANIZED GLASS

Jonatas U. Nascimento[1], Giovana C. Zambuzi[1], João O. Ferreira[1], Julia H. Paula[1], Tatiana S. Ribeiro[1], Adriano L. Souza[1], Cécile A. Dreiss[2], Lucimara L. Silva[3], Kelly R. Francisco[1,*]

[1] Department of Natural Science, Mathematics and Education, Federal University of São Carlos – UFSCar, Rodovia Anhanguera km 174. CEP: 13604-900. Araras - SP, Brazil.

[2] King's College London, Institute of Pharmaceutical Science, Franklin-Wilkins Building, 150 Stamford Street, SE1 9NH, London, UK.

[3] Chemical Engineering Course, Federal Technological University of Paraná - UTFPR, Estrada dos Pioneiros, 3131 - Jardim Morumbi. CEP: 86036-370. Londrina - PR, Brazil.

* corresponding author. E-mail: kfrancisco@ufscar.br

Abstract

Layer-by-layer (LbL) techniques are strategically important to obtain highly organized and oriented materials. Understanding film formation and nanoscale structures at the interface is important for many biological, industrial and technological processes. We describe a LbL film formed from a silanized glass surface coated with high-methoxyl pectin. The chemical composition of the surfaces was characterized by X-ray photoelectron spectroscopy (XPS); surface topology and chemistry were analyzed by Atomic Force Microscopy coupled with Infrared Spectroscopy (AFM-IR). Varying pH and concentration of the casting pectin solutions results in surfaces with different wettability, measured by contact angle. At high pH, pectin chains are highly charged, resulting in chain repulsions, poor coverage and low wettability due to exposure of the silane chains. At higher concentration, chains extend from the surface and wettability increases. This work establishes a facile route towards value-added materials from pectin, establishing clear links between wettability, nanostructure and composition at the interface.

Keywords: pectin, silanized glass, pH, layer-by-layer, wettability

1. Introduction

Self-assembled monolayers (SAMs) and layer-by-layer (LbL) techniques provide organized thin films by adsorption of negative and positive electrolytes from a solution, forming alternative layers at a solid interface, producing uniform and stable coatings with very high surface coverage, controlled layer thickness, and minimizing nonspecific adsorption [1-4]. The development of robust methodologies for such coatings is extremely important for a myriad of applications [5-7], for instance as

sensors [8], medical implants [9] and cell transplantation therapy [10], lubrication [11], corrosion inhibition [12], surface patterning in photoresists [13], or the prevention of nonspecific adsorption and biofouling, and for the formulation of nanoparticulate systems with controlled encapsulation [14] and release properties [15].

Surface modification techniques have become a significant focus of materials research as they can transform inexpensive substrates into high added value functional products. Through them it is also possible to modify the wettability of a surface by transforming it, for example, from a superhydrophilic surface to a superhydrophobic one [16]. Polysaccharides are an attractive option to form films and coatings [17]; they are renewable, widely available, low-cost and can have their functional groups modified. They can be adsorbed or covalently anchored to surfaces, modifying them in a simple and versatile way [18-20], to improve adhesion [21], wettability [22], tribological behavior [11] or water and chemical resistance. In this context, the use of biopolymers in the production of films has gained prominence. Pectin, a high molecular weight polysaccharide, is the main component of plant cell walls, usually extracted from apple and citrus peels, with 10-15% and 20-30% in dry basis, respectively [15], is an attractive candidate in the development of these technologies as it cheap, widely available and eco-friendly. It is composed of three main polysaccharide domains: homoga-lacturonan (HG) - a linear polymer of α-D-galacturonic acid and its methyl esterified counterpart -, ramnogalacturonan I (RGI) and ramnogalacturonan II (RGII). The carboxyl groups of the galaturonic acid units can be esterified with methanol, or partially acetyl-esterified. Depending on the extent of esterification, pectin is classified as high methoxyl pectin (> 50% esterified carboxyl groups) or low methoxyl pectin (< 50% esterified carboxyl groups). Pectins are acid and water soluble, and mainly used as thickeners, gelling agents in jams and fruit juices, and stabilizers in dairy products [23].

Pectin has also shown potential in tissue engineering applications, by modulating the adhesion and activity of different cell types [24]; as a biodegradable, green alternative to traditional food packaging in films [25]; in nanofibrous mats for antibacterial applications [26] or in controlled release formulations, such as solid lipid nanoparticles [15]. However, the formation of pectin films using LbL technique is scarce in the literature, which has prompted the current study. Due to the presence of carboxyl groups, an increase in pH causes the pectin to become highly charged, adversely affecting its interaction and adsorption as a result of the strong electrostatic repulsions. However, we hypothesize that this may also have an impact on the wettability of surfaces modified by the polymer, and thus provide a facile route towards tunability.

In this work, multilayer films based on negatively charged pectin adsorbed on silanized glass were prepared and characterized. The physico-chemical properties of the silanized glass surfaces coated with pectin, including their chemical composition, morphology and wettability, were studied by a range of techniques: zeta potential, infrared spectroscopy (IR), atomic force microscopy (AFM), X-ray photoelectron spectroscopy (XPS) and measurement of contact angle, for pectin solutions prepared at three different pH (4, 7 and 10) and at 1, 2 and 3% w/w. We demonstrate that the different conditions used allow the manipulation of surface properties through pH and concentration, in particular wettability, which is sustained by a different extent of adsorption of the pectin chains, nanoscale morphologies and exposure of different chemical groups at the surface, which thus impact the hydrophilicity. These simply engineered films have potential as coatings, for instance for the development of biodegradable films in food packaging, a pressing environmental issue due to the accumulation of synthetic plastics resistant to degradation.

2. Experimental

2.1. Materials

Citrus pectin Genu® pectin type 105-RS from CP Kelco Brazil SA with degree of esterification (DE) of 69.7 % and HM-SAG grade USA-SAG of 148 was used throughout. Poly(dimethylsiloxane), bis (3-aminopropyl) terminated (M_n = 27,000 g/mol), ethanol PA, NaOH and HCl were supplied by Sigma-Aldrich. All chemicals were used as received and Milli-Q deionized water (resistivity: 18 MΩ cm) was used in all aqueous systems. Glass slides (3.0 cm × 1.0 cm) were acquired from Precision Glass Line and they were covered with a chrome layer of 20 nm followed by a 100 nm gold layer deposition using the conventional lithography technique for AFM-IR analysis.

2.2. Sample preparation

2.2.1. Solutions preparation

Solutions containing 1%, 2% and 3% (w/w) of citrus pectin were prepared at different pH by adding small amounts of NaOH or HCl 0.1 M (4, 7 and 10). Solutions were stirred for 3h and sonicated for 30 minutes using an ultrasonic bath (Ultronique, model Q3.8/40A) at room temperature in order to solubilize the pectin chains. Solutions of poly(dimethylsiloxane), bis (3-aminopropyl) terminated (PDMS) were prepared using 15 μL of PDMS and 50 mL of ethanol PA. Solutions of pectin were made by weight, and the percentages are expressed in % w/w, unless stated otherwise.

2.2.2. Layer-by-layer deposition of silane and pectin on glass surfaces

Glass slides (3 cm × 1 cm) with or without gold were used as substrates. Prior to silane and pectin deposition, glass slides were immersed in various solvents in order to clean their surface in an ultrasonic bath for 20 minutes, in the following order: water, acetone

and ethanol. Thin films of macromolecules on the glass surfaces were prepared by using a dip-coater (ND-R Rotatory Dip Coater, Nadetech Innovations). The layer-by-layer deposition of the polymer was performed as follows:

i. The glass slides (with or without gold) were immersed at 150 mm/min in PDMS solutions for 150 seconds. Then, they were removed and left to dry in the air at room temperature for 30 seconds;

ii. The silanized glass slides were submerged at 150 mm/min in a solution of pectin for 150 seconds. They were then removed and kept in the air for 30 seconds to dry;

iii. In order to remove the excess of pectin on the silanized glass surfaces, slides were immersed at 150 mm/min in MilliQ water for 30 seconds. They were then removed and left to dry for 30 seconds.

2.3. Methods

2.3.1. Zeta Potential

The zeta potential of pectin solutions was measured at room temperature using a Zetasizer Nano-ZS analyzer (Malvern Instruments, UK).

2.3.2. Fourier transform Infrared (FT-IR)

The FT-IR spectra of pectin in the solid state was obtained with a Bruker FT-IR spectrometer, using KBr pellets. IR spectra of pectin films produced by casting the solutions at 50ºC were obtained in the ATR (attenuated total reflectance) mode, using a ZnSe window. The spectra were obtained by accumulating 128 scans within the spectral range of 500 to 4000 cm^{-1} with a resolution of 4 cm^{-1}.

159 *2.3.3. Atomic Force Microscopy (AFM) and Atomic Force Microscopy coupled with*
160 *Infrared (AFM-IR)*

161 AFM-IR measurements of 3% pectin adsorbed on silanized glass surface at different pH
162 were performed on a NanoIR2 system from Anasys Instruments. Samples were scanned
163 in contact mode using a gold-plated silicon nitride probe (ContGB-G model,
164 BudgetSensors) with the radius of curvature < 25 nm, resonance frequency of 13 kHz
165 and force constant of 0.2 N/m. IR spectra were obtained in the range of 1530-1850 cm^{-1}
166 with a wavelength resolution of 4 cm^{-1}. All samples were prepared on a glass surface
167 covered by gold as it increases the cantilever response to the expansion of the sample.
168 AFM images were also obtained using a Park Systems Microscope, model NX-10 in a
169 non-contact mode using a NanoWorld Si probe tip (FMR model), with the radius of
170 curvature < 12 nm, resonance frequency and force constant values of 75 kHz and 2.8
171 N/m, respectively. All micrographs were acquired at room temperature at 20% relative
172 humidity. Three different areas for each sample were scanned and the images were
173 treated using Gwyddion software.

174

175 *2.3.4. X-ray Photoelectron Spectroscopy (XPS)*

176 Pectin adsorbed on silanized glass surfaces were analyzed by XPS (Thermo Scientific
177 K-Alpha equipment) using the aluminum Kα line and a VG-CLAMP-2 electron
178 hemispherical analyzer, with a resolution of 0.85 eV and spot size value of 400 μm. The
179 atomic composition of the samples was calculated by integrating the peaks using
180 Thermo Scientific™ Avantage™ software.

181

182 *2.3.5. Contact angle*

Contact angles of 10 µL water droplets deposited on silane and pectin chains on glass surface were measured by the Young-Laplace method (sessile drop fitting) on Attension Theta Optical Tensiometer (Biolin Scientific). All measurements were made in duplicates from different glass surfaces and three different regions of each. Only the contact angle at the initial time (t = 0 s) was considered.

3. Results and Discussion

3.1. Zeta (ζ) Potential

Zeta potential measurements on the pectin solutions show that, over the range of pH values studied, pectin solutions had a negative charge (Table 1). Pectin is a weak polyanion with a pKa of about 3.6, above which it is deprotonated [27] and presents a net negative electric charge. The low pKa value is due to galactoronic acid, a weak acid found in the pectin structure [28]. At low pH, the anionic character of pectin chains is reduced due to the protonation of the carboxylic groups [29].

Table 1. ζ-potentials of pectin solutions at different pH values and concentrations.

Sample	**ζ-Potential / (mV)**		
pH value	**1%**	**2%**	**3%**
pH 4	- 29,7 ± 0.5	- 33,1 ± 2.6	- 31,4 ± 2.2
pH 7	- 38,8 ± 0.2	- 44,1 ± 3.1	- 40,9 ± 3.5
pH 10	- 38,0 ± 1.3	- 49,7 ± 4.4	- 48,1 ± 4.8

Increasing the pH value from 4 to 10 results in an increase in the negative charge of the polysaccharide chains, and thus an increase in the charge density. As a result, the zeta potential becomes more negative and the electrostatic repulsions between the pectin chains reach a maximum, resulting in an optimized stability of the macromolecules.

Similar values of the zeta potential have been reported by Maciel et al. [30] at pH 4 and 0.5% ($\zeta = -28.23 \pm 1.30$ mV) and by Freitas et al. [31] and Zhao et al. [32] at 0.01% ($\zeta \sim -17.5$ mV) and 0.05% ($\zeta = -12.80 \pm 1.43$ mV).

FT-IR analysis of pectin samples

The FT-IR spectra of the films formed by pectin solutions (3%) at pH values of 4, 7 and 10 were measured in order to identify the chemical stability of the pectin chains as a function of pH (Fig. 1).

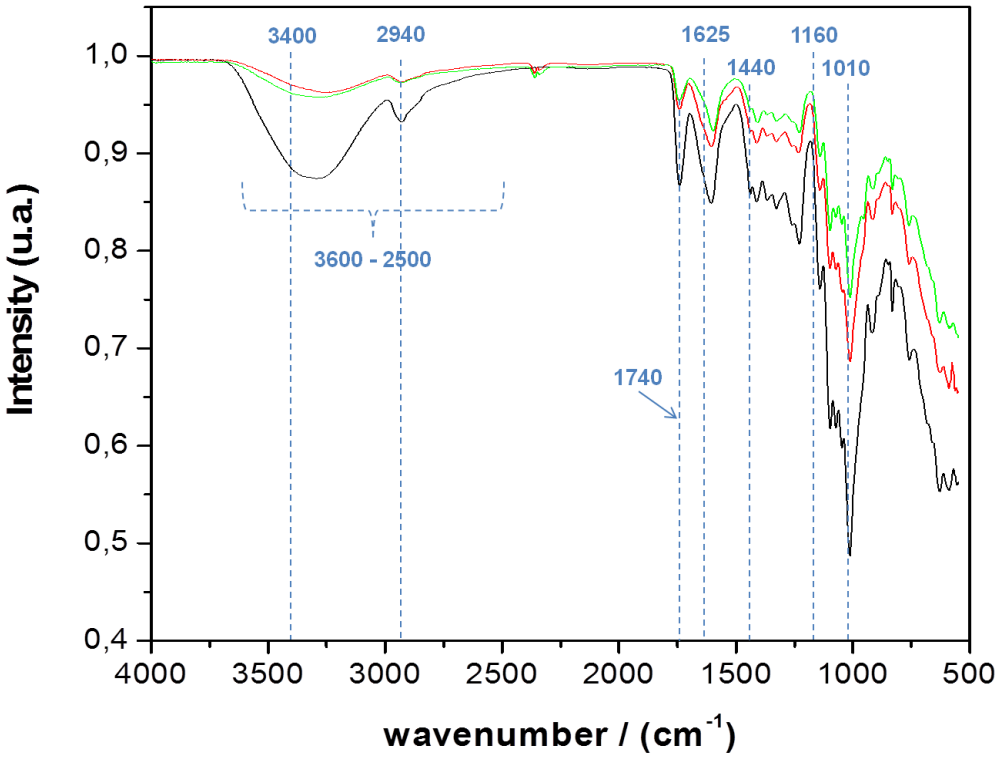

Figure 1: Infrared spectra of pectin films formed by an aqueous solution at 3% (w/w) with pH values of: pH 4 (black line), pH 7 (red line) and pH 10 (green line).

IR spectra of the pectin films presented a large band around 3400 cm^{-1} associated with the stretching of hydroxyl groups due both to the pectin chemical

structure and hydration with water molecules. The weak band at approximately 2900 cm^{-1} is associated to the C-H stretching. Bands around 1740 cm^{-1}, 1625 cm^{-1} and 1440 cm^{-1} are related to the stretching vibration of carboxylic groups (C=O ester), and the symmetric and asymmetric stretching of COO^{-}, respectively. Bands at 1160-1010 cm^{-1} are attributed to the C-O-C (ether) and rings C-C bonds of galacturonic acid [33]. IR spectra show no structural modification of pectin chains dried at different values of pH, in agreement with other studies [26, 34, 35].

AFM and AFM-IR images of thin film surfaces

The topography of the bare glass and the gold-on-glass substrates used in this work are provided on the Supplementary Material (S. M. Figure 1). The silane chains on the glass surface (Fig. 2 *a*) comprises agglomerated polymeric chains and nanopores, randomly dispersed and leading to a rough surface, with root mean squared (rms) roughness of 1.3 nm and average value of 4.9 nm, respectively. The adsorption of pectin on these surfaces leads to different patterns, depending on the pH: at pH 4 (Fig. 2 *b*), smaller spherical particles and a smoother surface are obtained, compared to the pectin macromolecules adsorbed at higher pH (Fig. 2 *c*), where aggregates of a conical shape are visible. Rms and average values are 0.7 nm and 2.5 nm for pectin at low pH, and 2.0 nm and 4.6 nm for the chains at pH 10, respectively. Other surface areas were investigated, and the list of the main Multi-measurement average results are shown on the Supplementary Material (S.M. Table 1). These results suggest that at low pH (pH 4) pectin chains form a more compact layer on the silanized glass surface in comparison to higher pH (pH 10). An excess of negative charge at high pH (Table 1), leading to repulsion between the chains, may be responsible for an expansion away from the surface, so then explaining the higher rms values obtained on this surface.

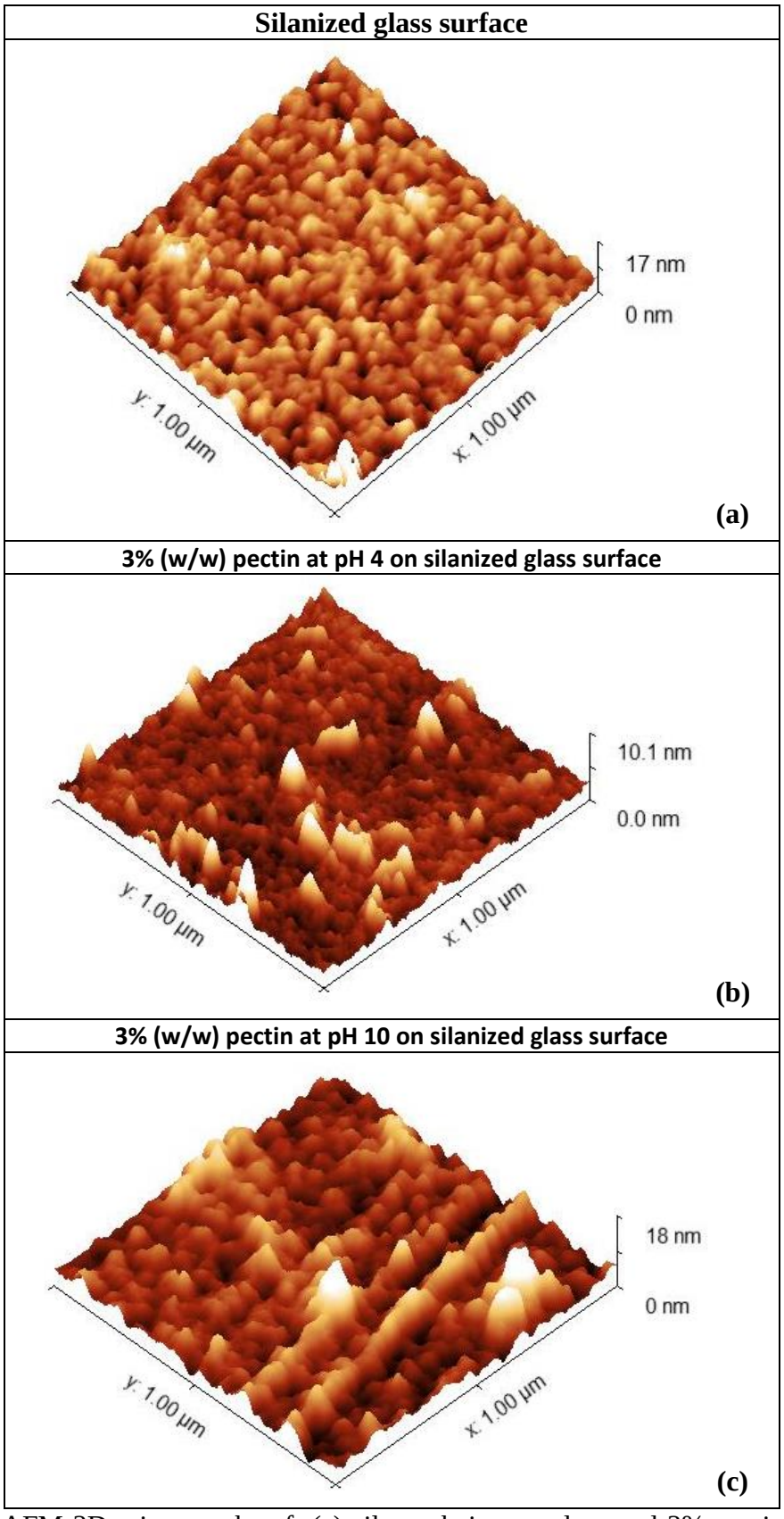

243 Figure 2: AFM 3D-micrographs of: (a) silane chains on glass and 3% pectin adsorbed
244 on silanized glass surface at (b) pH 4 and (c) pH 10.

Figure 3 *a*, *b*, *c* and *d* shows AFM-IR topological micrographs (top left) and chemical surface maps (top right) scanned at 1660 cm^{-1} and 1744 cm^{-1} for the silane film and the pectin adsorbed on silanized glass surfaces, respectively. The IR spectra obtained over different areas on the surfaces are also shown (bottom), with spatial resolution ≤ 50 nm.

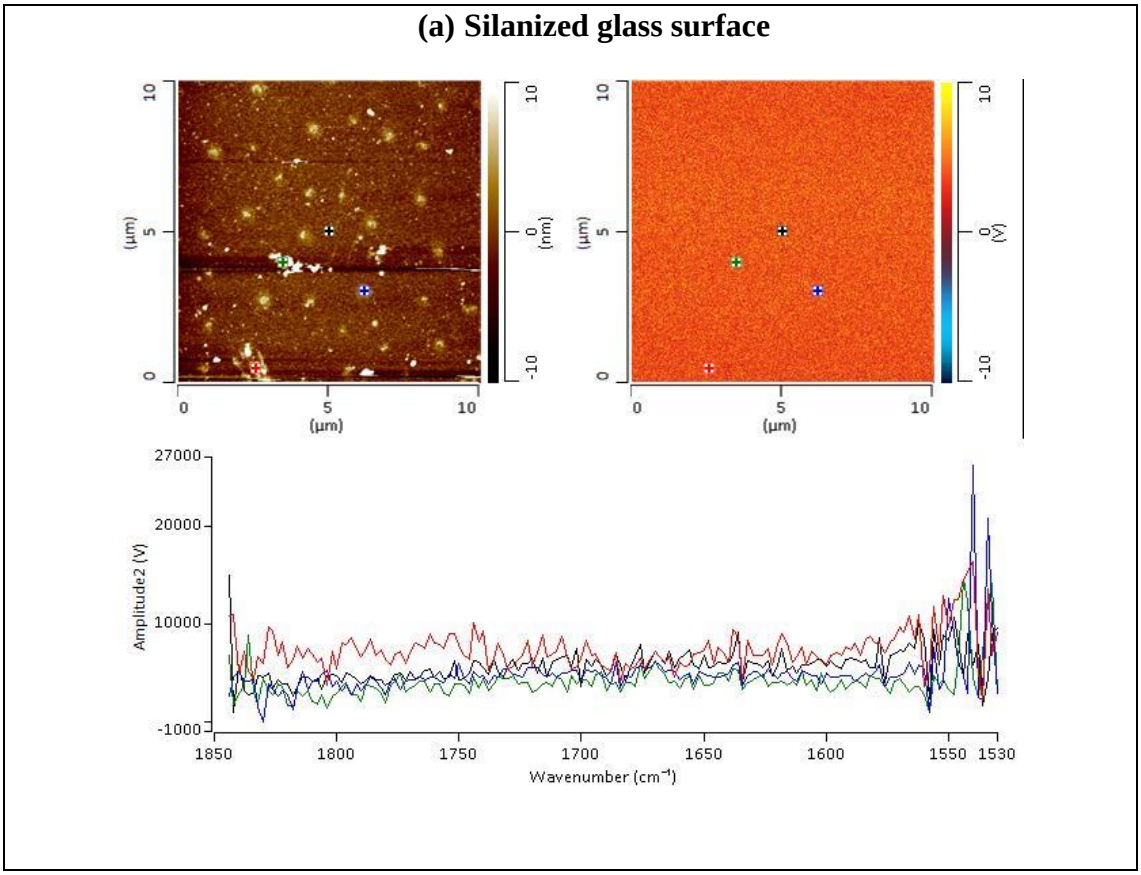

(b) 3% (w/w) pectin at pH 4 on silanized glass surface

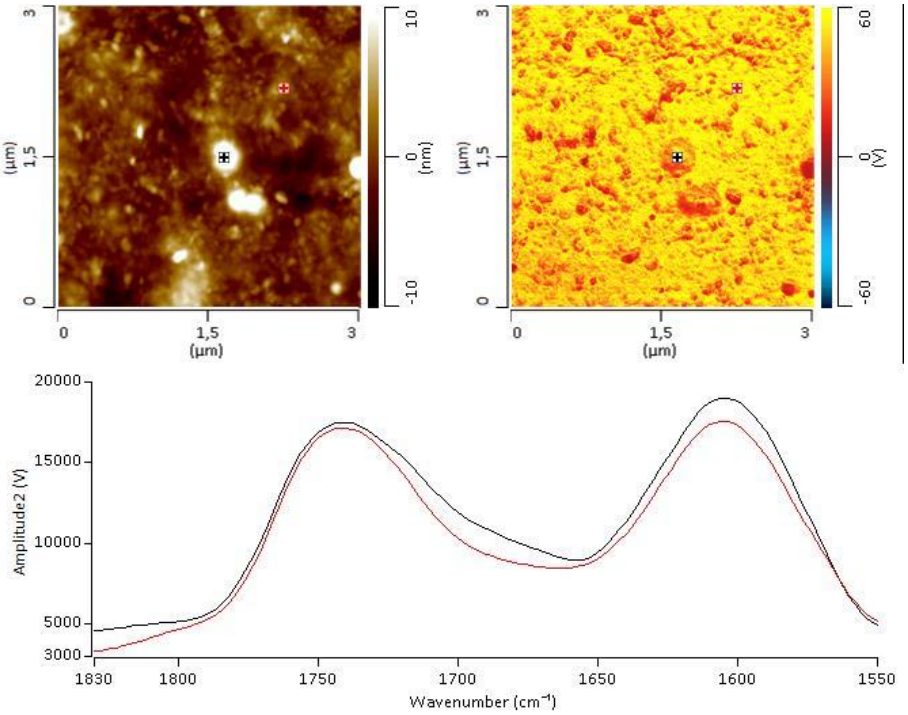

(c) 3% (w/w) pectin at pH 7 on silanized glass surface

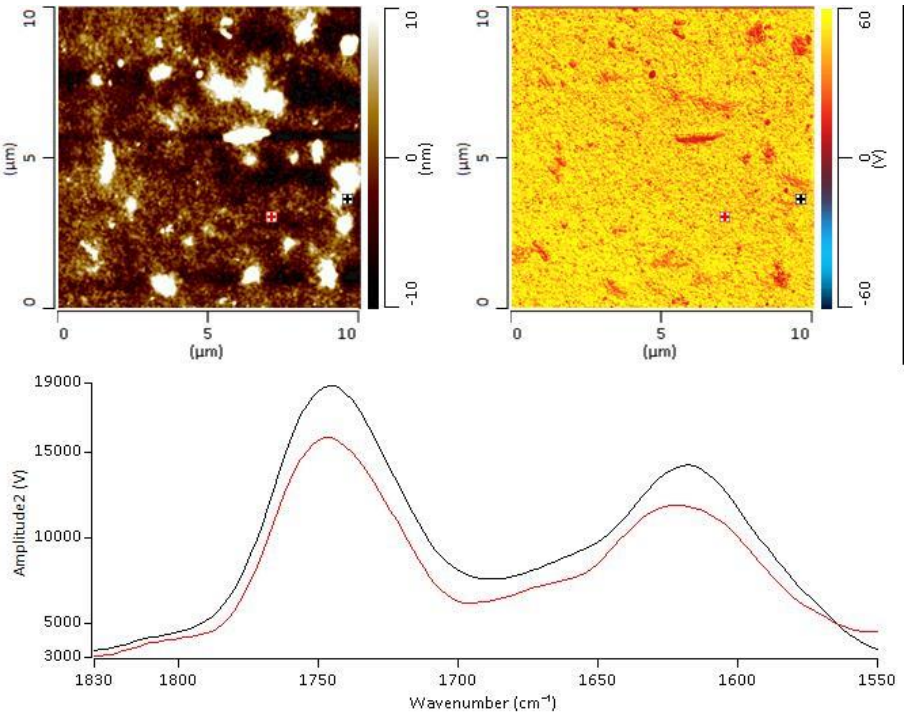

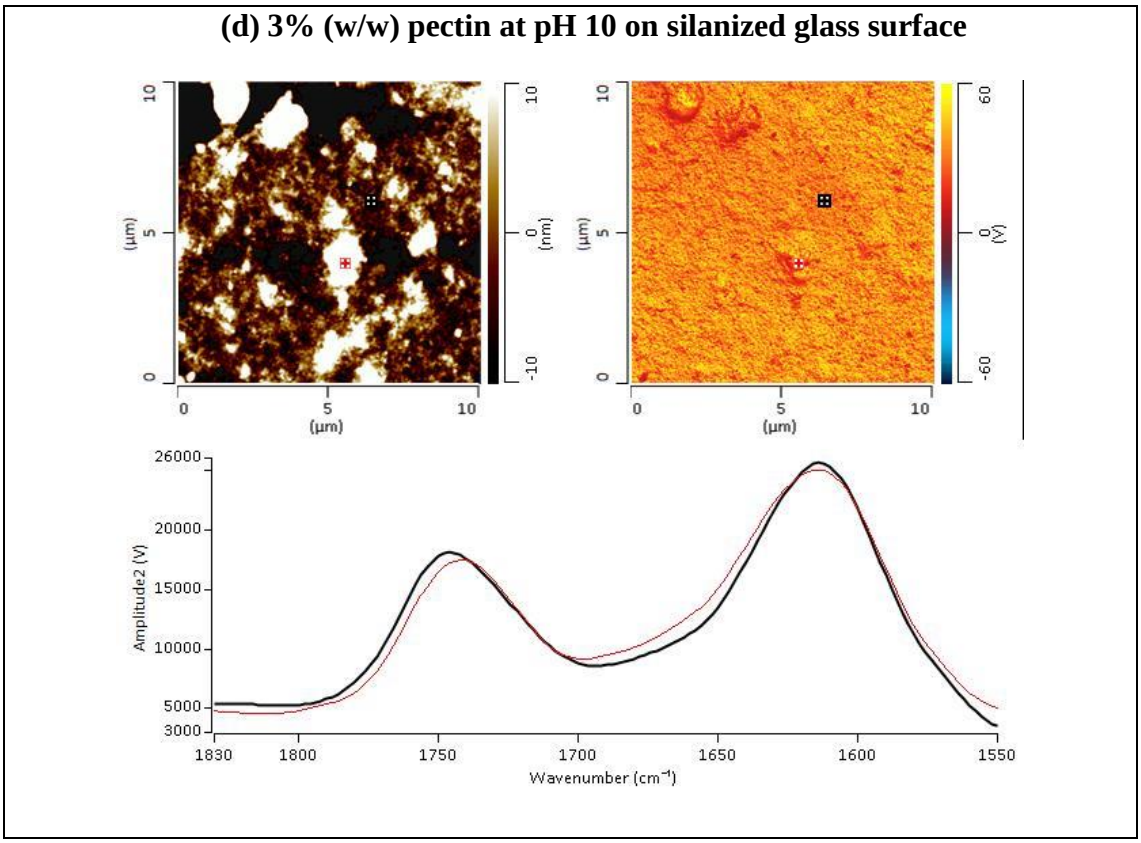

Figure 3: AFM-IR topography image (top left), AFM-IR chemical mapping (top right) and AFM-IR spectra in different regions (bottom) of: (a) silane chains on glass; 3% (w/w) pectin on silanized glass surface at (b) pH 4, (c) pH 7 and (d) pH 10.

The AFM images of the silane chains on the glass surface (Fig. 3 a) reveal micro and nanoaggregates homogeneously distributed on the surface, with rms and average value of 3.9 nm and 8.7 nm, respectively (Fig. 3 *a*, top left). The resulting chemical image (Fig. 3 *a*, top right) shows a surface homogeneously covered with an amplitude value approximately null for IR scanned at 1660 cm^{-1}, suggesting that the amine groups of the silane interact mainly with Si-OH sites of the glass rather than with the air. Furthermore, IR spectra in the range 1530 - 1850 cm^{-1} taken at three different positions (Fig. 3 *a*, bottom) show no absorption peak, confirming that C-H groups are exposed to the air as expected for a hydrophobic surface [36-38].

The topography images for silanized glass surfaces covered with pectin chains at different pH values (Fig. 3 *b*, *c* and *d*, top left) show rough surfaces with pores and polymeric aggregates, with rms values of 2.9 nm, 6.5 nm and 18.9 nm and average value of 6.9 nm, 13.5 nm and 33.3 nm at pH 4, 7 and 10, respectively. The chemical maps scanned at 1744 cm^{-1} (Fig. 3 *b*, *c* and *d*, top right) present a heterogenous distribution of the carboxylic groups (C=O ester). The surfaces covered with pectin at pH 4 present small agglomerates with C=O groups randomly distributed in an ester chemical environment. Pectin chains adsorbed at pH 7 display a more homogeneous surface, in which carboxylic groups are more in contact with the air in comparison with the lower pH. Surfaces covered with the biopolymer at pH 10 show the weakest signal from the carboxylic group absorption.

The relation between the IR intensity areas of esterified (C=O stretching at 1744 cm^{-1}) and deprotonated symmetric (COO^- stretching at 1612 cm^{-1}) bands can be related to the degree of esterification (DE) in pectin chains [39-41]. Analysis of the IR spectra (Fig. 3 *b*, *c* and *d*, bottom) yield DE values of 50 %, 62 % and 35 % for pectin chains adsorbed on silanized glass at pH 4, 7 and 10, respectively. This result suggests that the ester groups are predominantly in contact with the air for the surfaces prepared with pectin at pH 7, while deprotonated groups of the pectin structure are exposed to air at pH 10.

At lower pH, pectin chains have a lower negative charge density, and both C=O and COO^- groups are randomly distributed at the surface. As the pH value increases, negative charge also increases, but, at pH 7, the results suggest that the charge due to COO^- groups is mostly in the bulk while C=O is exposed to the air, in order to decrease the interfacial tension between the macromolecule layers and air. As the pH increases to

10, negative charge increases further, repulsions between chains are stronger and COO^- groups are more exposed to the air.

XPS analysis of the surfaces

Representative low-resolution XPS spectra and chemical composition of the surfaces are shown in Fig. 4 and Table 2, respectively. The peaks of C1s, O1s, Si2p, N1s and Na1s are centered at a binding energy of 285, 532, 103, 400 and 1072 eV, respectively [42-44].

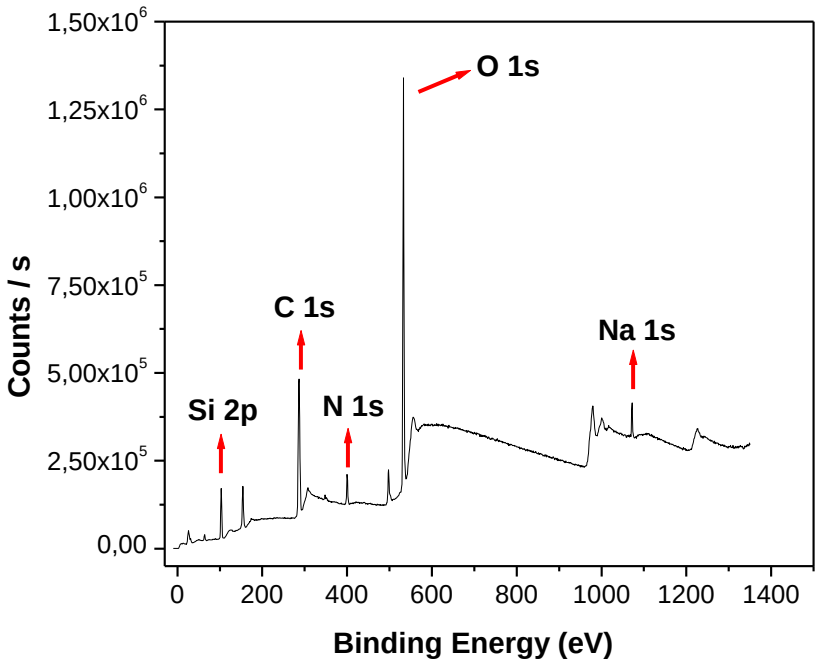

Figure 4: XPS spectrum of a silanized glass surface covered with 1% pectin at pH 7.

The formation of a pectin layer is confirmed by the change in Si/C ratio from 2.1 for the silane on glass to values below 0.4 in the presence of pectin. The lowest amount of adsorption is obtained at pH 10, and at the lowest concentration of pectin studied (1 %), probably due to the electrostatic repulsions between pectin chains at that pH and also between pectin and silane chains. At increasing concentrations of pectin, the Si

content decreases while the amount of C increases, demonstrating a better coverage with the biopolymer, which is optimum at the highest pectin concentration (3%) and pH 4, where Si decreases from 10.3% to 0.5%. The slight increase in nitrogen on the surface after pectin adsorption may be attributed to residual proteins from the biopolymer extraction, as suggested by Gadenne et. al. [45].

Table 2: Atomic composition of polymeric chains on glass surfaces.

1% (w/w) pectin on silanized glass				
Atom	**Atomic %**			
	Silanized Glass	**pH 4**	**pH 7**	**pH 10**
O 1s	50.1	32.6	36.9	27.8
Si 2p	31.3	10.3	12.4	18.4
C 1s	14.9	51.9	45.4	49.1
N 1s	0.5	2.9	4.2	3.1
Na 1s	1.3	1.3	1.7	0.7
2% (w/w) pectin on silanized glass				
Atom	**Atomic %**			
	Silanized Glass	**pH 4**	**pH 7**	**pH 10**
O 1s	50.1	34.9	32.6	36.2
Si 2p	31.3	3.4	4.1	4.7
C 1s	14.9	56.3	58.1	53.2
N 1s	0.5	3.7	4.0	4.0
Na 1s	1.3	1.7	1.2	2.0
3% (w/w) pectin on silanized glass				
Atom	**Atomic %**			
	Silanized Glass	**pH 4**	**pH 7**	**pH 10**
O 1s	50.1	34.0	34.0	30.9
Si 2p	31.3	0.5	2.5	5.0
C 1s	14.9	59.8	57.6	59.1
N 1s	0.5	3.5	4.6	3.9
Na 1s	1.3	1.7	1.4	1.2

The high-resolution C 1s spectra of the glass surfaces covered with layers of silane and pectin chains are shown in Fig. 5.

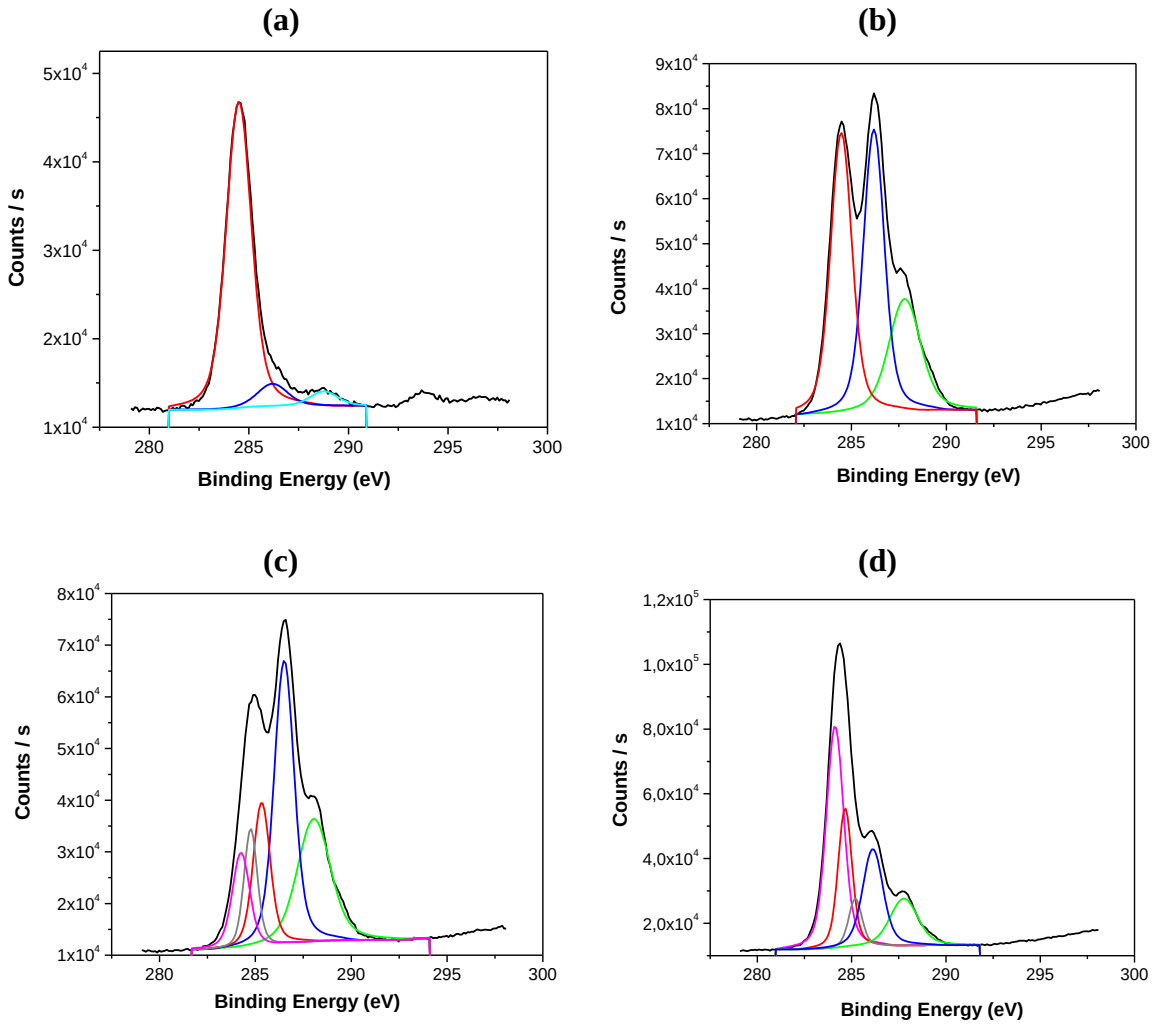

Figure 5: C1s core-level spectra of (a) silanized glass surface covered with 1% (w/w) pectin at (b) pH 4, (c) pH 7 and (d) pH 10.

The C 1s core-level spectra of silane glass surfaces covered with 1% pectin can be fitted by a combination of five different peaks at 284.0, 284.5, 286.2, 287.8 and 288.7 eV, attributed to the C-Si, C-C and C-H, C-O (or C-N), C=O and O-C=O species, in that order [46-48]. The C1s binding energies related to C-Si, C-C and C-H chemical environments were simplified by centering the peak at 285.0 eV, as shown in Table 3. The results indicate that the C-C (or C-H and C-Si) species at 285 eV for surfaces

covered with pectin at low concentration increase with an increase in pH, evidencing the lower adsorption of the biopolymer at pH 10, which thus results in a larger exposure of the silane macromolecules on the surface.

Table 3: XPS C1s parameters of the polymeric films on the glass surface.

1% (w/w) pectin				
Binding Energy (eV)	**Contribution (%)**			
	Silanized Glass	**pH 4**	**pH 7**	**pH 10**
285.0 (Si-C, C-C, C-H)	87.7	38.7	46.1	66.2
286.2 (C-0)	7.7	38.4	39.9	20.4
287.8 (C=O)	Nd	22.9	14.0	13.4
288.8 (O-C=O)	4.6	Nd	Nd	Nd
2% (w/w) pectin				
Binding Energy (eV)	**Contribution (%)**			
	Silanized Glass	**pH 4**	**pH 7**	**pH 10**
285.0 (Si-C, C-C, C-H)	87.7	24.3	28.7	27.6
286.2 (C-0)	7.7	53.5	46.2	37.0
287.8 (C=O)	Nd	18.7	25.0	9.8
288.8 (O-C=O)	4.6	Nd	Nd	7.04
3% (w/w) pectin				
Binding Energy (eV)	**Contribution (%)**			
	Silanized Glass	**pH 4**	**pH 7**	**pH 10**
285.0 (Si-C, C-C, C-H)	87.7	29.3	36.6	29.0
286.2 (C-0)	7.7	44.7	41.5	49.0
287.8 (C=O)	Nd	23.3	19.3	19.2
288.8 (O-C=O)	4.6	Nd	Nd	Nd
289.1 (O-C=O, O-C=N)	Nd	2.7	2.6	2.8

Nd - Not detectable

329

330 *3.5. Contact angle*

331 At low concentration of pectin (1%), the contact angle for water droplets
332 deposited on the surfaces coated with 1% pectin solutions were found to increase with
333 pH (Figure 6). However, at increasing concentration of pectin (2% and 3%), this
334 behavior changes. A relationship can be established between contact angle and the
335 exposure of silane macromolecules on the surface, evidenced by C-C; C-H and C-Si
336 species in XPS measurements (Table 3), linked to less hydrophilic surface and
337 consequently, larger contact angles (Figure 6).

338

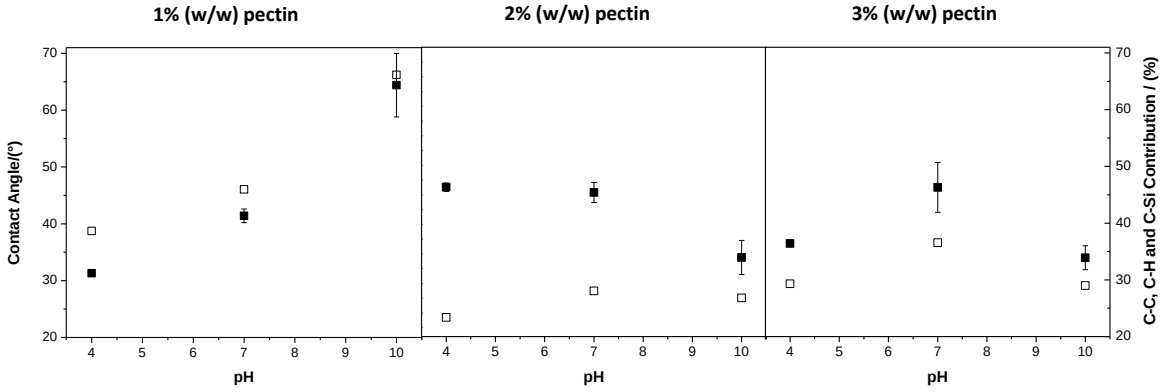

339

340 Figure 6: Contact angles (solid squares) and C-C, C-H and C-Si XPS contributions
341 (open squares) as a function of pH.

342

343 Based on these results, Figure 7 schematically presents the silane and pectin
344 chains on the glass surface as a function of pH for the two extreme concentrations, next
345 to the measured contact angles. At 1% and pH 4 the partially charged pectin chains are
346 strongly adsorbed on the silanized glass surface, as shown by XPS measurements.
347 Therefore, the adsorption of pectin on the glass surface covered with silane is probably

attribute to pectin-silane hydrophobic interactions, resulting in the exposure of the hydrophilic groups to the air and, consequently, an overall hydrophilic surface at this pH value. At higher pH, the pectin chains are more negatively charged, and the contact angle is higher, pointing to a lower adsorption of pectin on the silanized glass. At these high pH values (7 and 10), the higher negative charge density results in stronger electrostatic repulsions between adjacent pectin chains, which, consequently, are likely to avoid contact with each other, leading to the exposure of patches of hydrophobic silane.

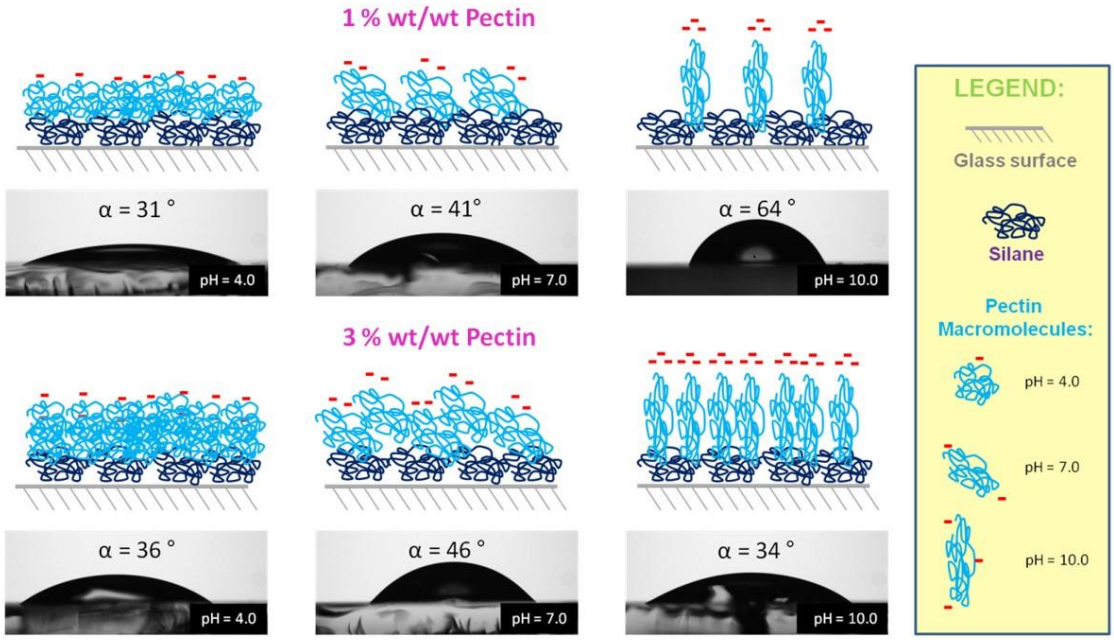

Figure 7: Scheme of the pectin chains assembled on the silanized glass surface.

The adsorption of the pectin chains on the glass surface at pH 4 at higher concentration (3%) is similar to the one obtained at 1%. At pH 7, the increase in contact angle is probably a consequence of the higher electrostatic repulsions between the chains and decreasing contact of COO^- groups with air. Steric interactions could also be contributing to the results of the contact angle, since the chains are expanded relative to the chains at pH 4. As a result, chains do not overlap perfectly, leaving void spaces

filled with air, and imparting overall a hydrophobic character to this coating. When the pH is increased to 10, the contact angle drops, which is attributed to the high charge density, imparting a high hydrophilicity to the surface. The drop in contact angle between 3% and 1% at this pH can be explained by a better coverage of the chains on the glass surface, reducing exposure of hydrophobic patches.

4. Conclusions

In this work, silanized glass surfaces coated with negatively charged pectin films were prepared and characterized. Adsorption of pectin films is stronger at pH 4 compared to pH 7 and 10, where the surface has a higher level of roughness, as revealed by AFM images. This simple process of modifying silanized surfaces, obtained by dip-coating with solutions prepared over a range of pH and concentrations, leads to surfaces with a range of wettabilities (all measurements provided contact angle values below 50°, with a single exception of 64°). Contact angle can be related to the results from XPS measurements, which gives the concentration of C-C, C-H and C-Si species at the surface, revealing the exposure of hydrophobic moieties. At low pH and with a 1% pectin solution, the adsorption of the polysaccharide is quite homogeneous, leading to a largely hydrophilic surface with contact angle of 31°. At higher pH values (7 and 10), the pectin chains bear more negative charge, due to deprotonation of the COO^- groups, resulting in stronger electrostatic repulsions between the chains. As a consequence, the chains are further apart from each other, leading to the exposure of hydrophobic patches on the surface. At higher concentration of pectin (2% and 3%), the better coverage of the surface induces, at the highest pH (pH 10), a higher hydrophilicity (and thus a lower contact angle), due to the high charge density.

This study thus demonstrates a facile route towards tuning the wettability of surfaces by layer-by-layer deposition of pectin by simply varying the pH and the concentration over a narrow range. All the surfaces obtained in this work were hydrophilic (with contact angles ranging from 31 to 64°) and in future work we will endeavor to achieve hydrophobic surfaces with modification of the pectin chain itself or by using high-methoxyl pectin from other species.

Acknowledgements

The authors would like to thank funding agencies Fundação de Amparo à Pesquisa do Estado de São Paulo (FAPESP) (2017/20006-4, 2018/12146-3, 2015/24136-4 and 2016/21616-8) and Conselho Nacional Científico e Tecnológico (CNPq) (427253/2016-0). The authors thank the Brazilian Nanotechnology National Laboratory (LNNano) for the preparation of the glass substrates covered with gold (LMF), and for XPS (LMN) and AFM (LCS) analysis and the National Laboratory for Nanotechnology in Agriculture - LNNA Embrapa (from SisNANO Program - National System of Laboratories in Nanotechnology) for zeta potential facility. We would also like to thank Professor Edvaldo Sabadini for access to the Contact Angle equipment.

References

[1] G. Decher, Fuzzy Nanoassemblies: Toward Layered Polymeric Multicomposites, Science 277 (1997) 1232- 1237.

[2] Z. Tang, Y. Wang, P. Podsiadlo, N. A. Kotov, Biomedical applications of layer-by-layer assembly: from biomimetics to tissue engineering, Advanced Materials 18 (2006) 3203-3224.

[3] X. Zhang, Y. Xu, Z. Xuan, H. Wu, J. Shen, R. Chen, Y. Xiong, J. Li, S. Guo, Progress on the layer-by-layer assembly of multilayered polymercomposites: Strategy, structural control and applications, Progress in Polymer Science 89 (2019) 76-107.

[4] B. S. Shim, P. Podsiadlo, D. G. Lilly, A. Agarwal, J. Lee, A. Tang, S. Ho, P. Ingle, D. Paterson, W. Lu, N. A. Kotov, Nanostructured Thin Films Made by Dewetting Method of Layer-By-Layer Assembly, Nano Letter 7 (2007) 3266-3273.

[5] M. Reig, G. Bagdziunas, A. Ramanavicius, J. Puigdollersd, D. Velasco, Interface engineering and solid-state organization for triindole-based p-type organic thin-film transistors, Physical Chemistry Chemical Physics 20 (2018) 17889-17898.

[6] G. P. Hellmann, K. Venkatesan, M. Mayor, E. Lörtscher, Metallic nanoparticle contacts for high-yield, ambient-stable molecular-monolayer devices, Nature 559 (2018) 232-235.

[7] R. Azmi, S. Y. Nam, S. Sinaga, S. H. Oh, T. K. Ahn, S. C. Yoon, I. H. Jung, S. Y. Jang, Improved performance of colloidal quantum dot solar cells using high electric-dipole self-assembled layers, Nano Energy 39 (2017) 355-362.

[8] A. Markov, V. Maybeck, N. Wolf, D. Mayer, A. Offenhäusser, R. Wördenweber, Engineering of Neuron Growth and Enhancing Cell-Chip Communication via Mixed SAMs, ACS Applied Materials & Interfaces 10 (2018) 18507−18514.

[9] D. Y. Kim, S. A. Lee, D. G. Kang, M. Park, Y. J. Choi, K. U. Jeong, Photoresponsive Carbohydrate-based Giant Surfactants: Automatic Vertical Alignment of Nematic Liquid Crystal for the Remote Controllable Optical Device, ACS Applied Materials & Interfaces 7 (2015) 6195-6204.

[10] J. Suzuki, N. Nagai, M. Nishizawa, T. Abeb, H. Kaji, Electrochemical manipulation of cell populations supported by biodegradable polymeric nanosheets for cell transplantation therapy, Biomaterials Science 5 (2017) 216-222.

[11] Y. Taira, C. E. McNamee, Polysaccharide films at an air/liquid and a liquid/silicon interface: effect of the polysaccharide and liquid type on their physical properties, Soft Matter 10 (2014) 8558-8572.

[12] C. W. Yang, C. Liu, D. J. Lin, M. L. Yeh, T. M. Lee, Hydrothermal treatment and butylphosphonic acid derived self-assembled monolayers for improving the surface chemistry and corrosion resistance of AZ61 magnesium alloy, Scientific Reports, 7 (16910) (2017) 1-13.

[13] A. Magomedov, A. Al-Ashouri, E. Kasparavicius, S. Strazdaite, G. Niaura, M. Jošt, T. Malinauskas, S. Albrecht, V. Getautis, Self-Assembled Hole Transporting

Monolayer for Highly Efficient Perovskite Solar Cells, Advanced Energy Materials 8 (2018) 1801892-1801901.

[14] T. Ederth, T. Ekblad, M. E. Pettitt, S. L. Conlan, C. X. Du, M. E. Callow, J. A. Callow, R. Mutton, A. S. Clare, F. D. Souza, G. Donnelly, A. Bruin, P. R. Willemsen, X. J. Su, S. Wang, Q. Zhao, M. Hederos, P. Konradsson, B. Liedberg, Resistance of Galactoside-Terminated Alkanethiol Self-Assembled Monolayers to Marine Fouling Organisms, ACS Applied Materials & Interfaces 3 (2017) 3890-3901.

[15] T. Wang, Q. Hu, M. Zhou, Y. Xia, M. P. Nieh, Y. Luo, Development of ‘‘all natural” layer-by-layer redispersible solid lipid nanoparticles by nano spray drying technology, European Journal of Pharmaceutics and Biopharmaceutics 107 (2016) 273-285.

[16] X. Li, X. Du, J. He, Self-Cleaning Antireflective Coatings Assembled from Peculiar Mesoporous Silica Nanoparticles, Langmuir 26 (2010) 13528–13534.

[17] P. Cazón, G. Velazquez, J. A. Ramírez, M. Vazquez, Polysaccharide-based films and coatings for food packaging: A review, Food Hydrocolloids 68 (2017) 136-148.

[18] L. Peng, H. Li, Y. Meng, Layer-by-layer structured polysaccharides-based multilayers on cellulose acetate membrane: Towards better hemocompatibility, antibacterial and antioxidant activities, Applied Surface Science 401 (2017) 25–39.

[19] Y. Fang, J. Wu, Z. K. Xu, Dextransucrase-catalyzed elongation of polysaccharide brushes with immobilized mono-/di-saccharides as acceptors, Chemical Communications 51 (2015) 129-132.

[20] Y. Wang, M. Yang, J. Qian, W. Xu, J. Wang, G. Hou, L. Ji, A. Suo, Sequentially self-assembled polysaccharide-based nanocomplexes for combined chemotherapy and photodynamic therapy of breast cancer, Carbohydrate Polymers 203 (2019) 203-213.

[21] M. Bračič, O. Šauperl, S. Strnad, I. Kosalec, O. Plohl, L. F. Zemljič, Surface modification of silicone with colloidal polysaccharides formulations for the development of antimicrobial urethral catheters, Applied Surface Science 463 (2019) 889–899.

[22] A. Wali, Y. Zhang, P. Sengupta, Y. Higaki, A. Takahara, M. V. Badiger, Electrospinning of non-ionic cellulose ethers/polyvinyl alcohol nanofibers: characterization and applications, Carbohydrate Polymers 181 (2018) 175–182.

[23] M. M. Gutierrez-Pacheco, L. A. Ortega-Ramirez, M. R. Cruz-Valenzuela, B. A. Silva-Espinoza, G. A. Gonzalez-Aguilar, J. F. Ayala-Zavala, Combinational approaches for antimicrobial Packaging: Pectin and cinnamon leaf oil. In B. V., Jorge (Ed), Antimicrobial food packaging (pp. 609-617), San Diego: Academic Press, 2016.

[24] O. Guillame-Gentil, O. Semenov, A. S. Roca, T. Groth, R. Zahn, J. Vörös, M. Zenobi-Wong, Engineering the extracellular environment: strategies for building 2D and 3D cellular structures, Advanced Materials 22 (2010) 5443–5462.

[25] R. Villa-Rojas, A. Valdez-Fragoso, H. Mújica-Paz, Manufacturing methods and engineering properties of pectin-based nanobiocomposite films, Food Engineering Reviews 10 (2018) 46-56.

[26] T. Zhang, P. Zhou, Y. Zhan, X. Shi, J. Y. Lin, X. Li, H. Deng, Pectin/lysozyme bilayers layer-by-layer deposited cellulose nanofibrous mats for antibacterial application, Carbohydrate Polymers 117 (2015) 687-693.

[27] M. Bayarri, N. Oulahal, P. Degraeve, A. Gharsallaoui, Properties of lysozyme/low methoxyl (LM) pectin complexes for antimicrobial edible food packaging. Journal of Food Engineering 131 (20140 18-25.

[28] C. Rolin, Pectins and their manipulation, In C. Seymour, & P. Knox (Eds.), Commercial pectins preparation (pp. 222-241). London: Blackwell, 2002.

[29] T. Giancone, E. Torrieri, P. Masi, C. Michon, Protein–polysaccharide interactions: Phase behaviour of pectin–soy flour mixture, Food Hydrocolloids 23 (2009) 1263-1269.

[30] V. B. Maciel, C. M. P. Yoshida, T. T. Franco, Chitosan/pectin polyelectrolyte complex as a pH indicator. Carbohydrate Polymers, 132 (2015) 537-545.

[319] M. L. F. Freitas, K. M. Albano, V. R. N. Telis, Characterization of biopolymers and soy protein isolate-high-methoxyl pectin complex, Polímeros 27(1) (2017) 62-67.

[32] G. Y. Zhao, H. J. Diao, W. Zong, Nature of pectin–protein–catechin interactions in model systems: Pectin–protein–catechin interactions, Food Science and Technology International 19 (2) (2013) 153-165.

[33] S. B. Engelsen, L. Norgaard, Comparative vibrational spectroscopy for determination of quality parameters in amidated pectins as evaluated by chemometrics. Carbohydrate Polymers 30 (1996) 9-24.

[34] B. Sun, X. Zhang, G. Zhou, P. Li, Y. Zhang, H. Wang, Y. Xia, Y. Zhao, An organic nonvolatile resistive switching memory device fabricated with natural pectin from fruit peel, Organic Electronics 42 (2017) 181-186.

[35] E. Ansarifar, M. Mohebbi, F. Shahidi, A. Koocheki, N. Ramezanian, Novel multilayer microcapsules based on soy protein isolate fibrils and high methoxyl pectin: Production, characterization and release modeling, International Journal of Biological Macromolecules 97 (2017) 761-769.

[36] L. Zhou, S. Yin, Z. Guo, N. Yang, J. Li, M. Zhang, Y. Zheng, Multilevel nanoparticles coatings with excellent liquid repellency, Advanced Materials Interfaces 5 (2018) 1800405-1800412.

[37] P. H. P. Olívio, L. A. Correia, J. H. Paula, O. N. Oliveira Jr, A. L. Souza, Exploring electrochemical reactivity toward ametryn of hybrid silicate films with phosphomolybdic acid, Materials Science & Engineering B 229 (2018) 13-19.

[38] Y. Li, C Dai, X. Wang, W. Lv, H. Zhou, G. Zhao, L. Li, Y. Sun, Y. Wu, M. Zhao, A novel strategy to create bifunctional silica-protected quantum dot nanoprobe for fluorescence imaging, Sensors & Actuators: B. Chemical 282 (2019) 27-35.

[39] A. K. Chatjigakis, C. Pappas, N. Proxenia, O. Kalantzi, P. Rodis, M. Polissiou, FT-IR spectroscopic determination of the degree of esterification of cell wall pectins from stored peaches and correlation to textural changes. Carbohydrate Polymers 37 (1998) 395-408.

[40] M. Chylinska, M. Szymanska-Chargot, A. Zdunek, FT-IR and FT-Raman characterization of non-cellulosic polysaccharides fractions isolated from plant cell wall, Carbohydrate Polymers 154 (2016) 48-54.

[41] S. Talekar, A. F. Patti, R. Vijayraghavan, A. Arora, An integrated green biorefinery approach towards simultaneous recovery of pectin and polyphenols coupled with bioethanol production from waste pomegranate peels, Bioresource Technology, 266 (2018) 322-334.

[42] X. P. He, X. W. Wang, X. P. Jin, H. Zhou, X. X. Shi, G. R. Chen, Y. T. Long, Epimeric monosaccharide-quinone hybrids on gold electrodes toward the electrochemical probing of specific carbohydrate-protein recognitions, Journal of the American Chemical Society 133 (2011) 3649-3657.

[43] B. Schampera, D. Tunega, R. Šolc, S. K. Woche, R. Mikutta, R. Wirth, S. Dultz, G. Guggenberger, External surface structure of organoclays analyzed by transmission electron microscopy and X-ray photoelectron spectroscopy in combination with molecular dynamics simulations, Journal of Colloid and Interface Science 478 (2016) 188-200.

[44] S. Lee, E. Byeon, S. Jung, D. G. Kim, Heterogeneity of hard skin layer in wrinkled PDMS surface fabricated by ar ion-beam irradiation, Scientific Reports 8:14063 (2018) 1-8.

[45] V. Gadenne, L. Lebrun, T. Jouenne, P. Thebault, (2013). Antiadhesive activity of ulvan polysaccharides covalently immobilized onto titanium surface, Colloids and Surfaces B: Biointerfaces 112 (2013) 229-236.

[46] J. Hoypierres, V. Dulong, C. Rihouey, S. Alexandre, L. Picton, P. Thebault, Two methods for one-point anchoring of a linear polysaccharide on a gold surface. Langmuir 31 (2015) 254-261.

[47] F. Kara, E. A. Aksoy, Z. Yuksekdag, N. Hasirci, S. Aksoy, Synthesis and surface modification of polyurethanes with chitosan for antibacterial properties. Carbohydrate Polymers 112 (2014) 39-47.

[48] C. Nietzold, P. M. Dietrich, M. Holzweber, A. Lippitz, A. Kamalakumar, V. Blanchard, S. Ivanov-Pankov, W. Weigel, U. Panne, W. E. S. Unger, Surface chemical characterization of model glycan surfaces and shelf life studies of glycan microarrays using XPS, NEXAFS spectroscopy, ToF-SIMS and fluorescence scanning, Applied Surface Science 459 (2018) 860-873.